JOURNAL OF FOOD QUALITY & HAZARDS CONTROL
SHAHID SADOUGHI UNIVERSITY OF MEDICAL SCIENCES & HEALTH SERVICES

Journal of Food Quality and Hazards Control 11 (2024) 232-244

Producing Polycaprolactone and Basil Seed Gum Nanofibers Using an Electrospinning Process

N. Zamani [1], A. Farsad-Naeimi [1], E. Sharifi [2], V. Ghasemzadeh-Mohammadi [1*]

1. Department of Nutrition and Food Safety, School of Medicine, Hamadan University of Medical Sciences, Hamadan, Iran
2. Department of Tissue Engineering and Biomaterials, School of Advanced Medical Sciences and Technologies, Hamadan University of Medical Sciences, Hamadan, Iran

HIGHLIGHTS

- Basil Seed Gum (BSG) concentration was the most influential variable affecting the relative standard deviation of nanofiber diameter.
- BSG reduced the size and improved the texture of the nanofibers.
- BSG increased Water Vapor Permeability and reduced the Oxygen Transfer Rate.

Article type
Original article

Keywords
Polyesters
Ocimum basilicum
Nanofibers
Biopolymers.

Article history
Received: 30 May 2024
Revised: 10 Aug 2024
Accept: 30 Nov 2024

Abbreviations
AFM=Atomic Force Microscopy
ATR-FTIR=Attenuated Total Reflectance-Fourier Transform Infrared spectroscopy
BSG=Basil Seed Gum
BSM=Basil Seed Mucilage
FE-SEM=Field Emission-Scanning Electron Microscopes
OTR=Oxygen Transmission Rate
PCL=Polycaprolactone
PRESS=Prediction Residual Error Sum of Squares
RSDD=Relative Standard Deviation of nanofiber Diameter
TGA=Thermal Gravimetric Analysis
TS=Tensile Strength
WVP=Water Vapor Permeability

ABSTRACT

Background: Novel packaging materials often exhibit enhanced environmental sustainability, safety, and biodegradability compared to conventional plastics. This work aims to identify and improve key factors influencing the production of polycaprolactone (PLC)-Basil Seed Gum (BSG) nanofibers.

Methods: The optimization of electrospun nanofibers containing PLC and BSG was done using a Box-Behnken design. Four parameters were selected as independent variables: BSG concentration percentage (A), percentage of acetone in PLC solution (B), voltage (C), and distance from nozzle to collector (D). Two responses, namely the Relative Standard Deviation of nanofiber Diameter (RSDD) and Tensile Strength (TS), were chosen as dependent variables. Twenty-nine treatments were created using Design Expert software and Microsoft Excel (Design-Expert-Stat-Ease version 11 and Microsoft Excel 2012).

Results: it was found that variables A and D have the greatest effect on diameter distribution, while variables A and B have the most significant effect on TS. At a voltage of 15 kV, RSDD decreased as variable A increased from 10 to 25%. Subsequently, this trend increased from 25 to 40%. Increasing variable A from 10 to 25% at each distance (D) resulted in a decrease in RSDD, followed by an increase from 25 to 40%. TS rose as variable A declined from 40 to 25%, after which a decline was observed.

Conclusion: BSG both reduced the size and improved the texture of the nanofibers, as well as enhancing the performance of Oxygen Transmission Rate. Furthermore, BSG negatively affected the thermal stability of films in the Thermal Gravimetric Analysis-Differential Thermal Analysis. A detrimental impact on Water Vapor Permeability was observed when combining these two compounds. The mechanical qualities generally decreased with the addition of BSG.

* Corresponding author (V. Ghasemzadeh-Mohammadi)
E-mail: v.gh-mo@umsha.ac.ir
ORCID ID: https://orcid.org/0000-0002-1858-3297

To cite: Zamani N., Farsad-Naeimi A., Sharifi E., Ghasemzadeh-Mohammadi V. (2024). Producing polycaprolactone and basil seed gum nanofibers using an electrospinning process. *Journal of Food Quality and Hazards Control*. 11: 232-244.

DOI: 10.18502/jfqhc.11.4.17441 Journal website: http://jfqhc.ssu.ac.ir

[DOI: 10.18502/jfqhc.11.4.17441]

Introduction

Packaging serves several functions, including customer engagement, product protection, manufacturing facilitation, enhancement of user-friendliness, and optimization of consumer time efficiency (Wandosell et al., 2021). Food packaging protects food from chemical, physical, and biological contaminants while maintaining the quality and safety of food products. According to estimates, food packaging accounts for over 33% of the global market (Nemat et al., 2019). Biopolymers exhibit greater structural diversity and variability, and chemical composition, providing researchers with a wide range of options to customize the characteristics of the final packaging material (Mittal, 2011). These novel packaging materials often exhibit improved environmental sustainability, safety, and biodegradability compared to conventional plastics. Numerous studies have approved the application of various biodegradable polymers, such as Polylactic Acid (PLA), Polycaprolactone (PCL), Poly 3-Hydroxybutyrate-co-3-hydroxyvalerate (PHBV), starch, chitosan, and polysaccharides, as barrier coatings for food packaging materials (Adibi et al., 2023; Lo Faro et al., 2023). PCL is a polymer that exhibits flexibility and biodegradability due to its low melting temperature and elongation properties. This polymer is a synthetic semi-crystalline material that is biodegradable. It has a melting point of around 60 °C and a glass transition temperature of around -60 °C (Lo Faro et al., 2023; Thakur et al., 2021). PCL provides excellent resistance to water, oil, solvent, and chlorine in the resulting polyurethane.

Biomass-derived polymers include a range of compounds such as polysaccharides, proteins, lipids, peptides, polyhydroxyalkanoates, and gums. These polymers are produced from plants, animals, and microbes through fermentation or chemical processes. Utilizing mucilages in the production of biodegradable films offers several benefits. Mucilages are cost-effective in comparison to the majority of biopolymers. Their extraction is straightforward and yields a high quantity (Jouki et al., 2013). Moreover, mucilages are renewable and derived from natural sources, and they enhance the barrier properties of films by preventing moisture and oxygen movement. Mucilage can also extend the shelf-life of final products by incorporating bioactive ingredients (Beikzadeh et al., 2020).

In recent years, mucilage has emerged as a novel biopolymer resource for the manufacturing nanofibers (Sen et al., 2022). Certain seeds, like basil seeds, contain substantial quantities of mucilage. Basil, scientifically known as *Ocimum basilicum* L. var. *thyrsiflora*, belongs to the *Ocimum* genus within the *Lamiaceae* family. It is mostly recognized for its seeds, which are small, ebony-colored, and elliptical in shape. Basil seeds have demonstrated a satisfactory quantity of gum with favorable functional characteristics compared to those found in other commercially available food hydrocolloids (Mirhosseini and Amid, 2012).

Additionally, it has a low manufacturing cost (Hashemi Gahruie et al., 2017). Numerous methodologies have been used to fabricate thin polymer matrices for packaging purposes including solvent casting, extrusion, thermoforming, and compression molding. Electrospinning technology enables precise manipulation of the end product's size, porosity, and mechanical properties, as well as the incorporation of bioactive compounds (Min et al., 2022). Response Surface Methodology (RSM) is a collection of mathematical and statistical methodologies used to construct empirical models and elucidate the associations between numerous inputs and their corresponding responses (Biswas et al., 2019). A system (such as an industrial process, analytic technique, or synthesis) operates frequently under specific parameters. Researchers consider the potential to enhance outcomes by modifying the values of these governing parameters. This involves investigating a permissible area within the parameter space where variation occur (Sarabia and Ortiz, 2009). The Box-Behnken Design (BBD) is an effective strategy for response surface approach due to its ability to: (i) estimate parameters of quadratic model, (ii) construct ordered designs, (iii) identify the lack of fit in the model; and (iv) utilize blocks (Ferreira et al., 2007). This work aims to develop and optimize critical variables in manufacturing PCL-Basil Seed Gum (BSG) nanofibers.

Materials and methods

Materials

PCL powder (molecular weight=80,000), acetic acid (glacial, ReagentPlus®, ≥99%), acetone, and formic acid (98-100%, EMPLURA®) were obtained from Sigma-Aldrich, St. Louis, USA. Basil seeds were purchased from local stores in Hamadan, Iran.

BSG extraction and purification

The basil seeds were immersed in a mixture of 1:70 distilled water, heated in a bain-marie (Shimiazma, Iran) at a temperature of 70 °C for 5 min. They were then mixed for five min using a low-speed mixer (Scientz, China), and centrifuged at 5,200 rpm for 10 min. The resulting gum was placed on the plate and dried at 50 °C in an incubator (Shimiazma, Iran). The remaining seeds were once again removed. The chilled powdered gum underwent purification using the Nazir process with some modifications (Nazir and Wani, 2021). One percent BSG solution in deionized water was prepared and stirred for 24

[DOI: 10.18502/jfqhc.11.4.17441]

h. The uniform solution was combined with 96% alcohol (Sigma-Aldrich, USA) in a ratio of 1:3, stirred for 2 h, and then centrifuged for 10 min at 5,000 rpm. The resin was dehydrated in a 50 °C incubator. For the following operation, the powder was stored at room temperature.

Preparation of solutions for electrospinning

A solution was prepared by dissolving one g of refined BSG in 100 ml of formic acid and stirring it with a Heater stirrer (Shimipajouh. Co, Iran) for 24 h; followed by a filtration to remove insoluble particles and contaminants. Next, 20 g of PCL was dissolved in 100 ml of a 60:40 acetic acid and acetone mixture and mixed for 6 h using a magnetic stirrer (Shimipajouh. Co, Iran). The PCL and BSG were then combined in various ratios according to the experimental design.

Electrospinning process

Nanofibers were prepared using dual-pump electrospinning equipment (HV35P OV, Iran). The collector consisted of a drum measuring 250 mm in length, rotating at a speed of 700 rpm. A syringe loaded the solution, which was then connected to an 18 G stainless steel needle. The electrospinning process was conducted under ambient conditions with the following parameters: an injection rate of one ml/h, a voltage of 18 kV, and a distance of 150 mm. The nanofibers that had gathered on the surface of the aluminum foil were separated and used for subsequent studies.

Measuring the diameter of nanofibers

Field Emission-Scanning Electron Microscopes (FE-SEM) was employed to investigate the surface morphology of the materials (TSCAN, Czech Republic) (Janani et al., 2020). The 1×4 mm sheets were attached using carbon glue and then coated with a layer of gold prior to inspection. The ImageJ software (version 1.52) was used to calculate nanofibers' average diameter.

Tensile Strength (TS) and thickness

Firstly, the film thickness was measured using a micrometer (Mitutoyo Corporation, Kawasaki, Japan) at three randomly selected sites on each sample with the measurement precision of 0.001 mm. The TS of the sheets was measured with a texture analyzer (STM-20, Santam Co, Iran). One strip was used to measure 100 by 30 mm. Ten mm of film was stretched each minute while positioned between the machine clamps.

Atomic Force Microscopy (AFM)

The surface morphology and roughness of the films were determined using AFM (ND-MDT, Russia) on the 3D picture (Suganthi et al., 2020).

Thermal Gravimetric Analysis-Differential Thermal Analysis (TGA-DTA)

The Ramp method was employed using n Simultaneous Differential Thermal Analysis (SDT) Q600 instrument (Artisan Technology Group, USA) to conduct TGA-DTA analyses. For this purpose, the samples were heated from 40 to 500 $^{\circ}$C with a heating rate of 10 $^{\circ}$C/min under an argon atmosphere.

Attenuated Total Reflectance-Fourier Transform Infrared spectroscopy (ATR-FTIR)

The samples were analyzed using ATR-FTIR spectrometry (AVATAR 370, Thermo, USA) with a spectral resolution of four 1/cm between 600 and 4,000 1/cm. The spectra were processed using OPUS spectral analysis software (OPUS 8.0) (Pan et al., 2019).

Oxygen Transmission Rate (OTR)

OTR of the films was measured according to standard ISO 15105-1:2007 (ISO, 2007). The film specimens, with a diameter of six mm, were subjected to an oxygen pressure of 50 mbar; the flow rate through them was documented.

Water Vapor Permeability (WVP)

WVP in the films was quantified using the gravimetric method (ASTM International, 2005). Film samples were placed in a container of calcium chloride ($CaCl_2$) until they reached a state of uniform mass. Subsequently, the film sections were meticulously placed onto the cap of vials containing $CaCl_2$ and maintained at a relative humidity of 70%. The vials underwent weight measurements at 24 h intervals. A graphical representation of weight variations over time was generated and calculated. The researchers employed the WVP rate tester to observe and measure the rate of water loss in the vials over time. Steady-state values were then computed using equations 1 and 2:

$WVTR\ (g/m^2/24\ h)=S/A$

Eq 1

$WVP\ (g/m^1.s^1.Pa^1)=WVTR\times X/\Delta P$

Eq 2

Where S is the slope by a linear regression, A is the film transfer surface, X is the average film thickness (m), and ΔP is the pressure difference (Pa) (Cazón et al., 2022).

Model optimization quality

The efficiency of the polynomial model's fit was indicated by the coefficient determination R^2 and R^2_{adj} (Mohammadi et al., 2013). The Prediction Residual Error Sum of Squares (PRESS) measures how the model fits each point in the design. Its value is expressed as the sum of squares of the PRESS residuals and can be used to compute an R for prediction (Myers et al., 2016).

[DOI: 10.18502/jfqhc.11.4.17441]

Optimization

Four variables, including the percentage of BSG (A) (10-25-40%), the percentage of acetone as a solvent in the PCL solution (B) (20-40-60%), the voltage of the electrospinning instrument (C) (15-20-25), and nozzle distance to the collector (D) (12-15-18), were optimized using Behnken's Box design (Ferreira et al., 2007).

The software (Design Expert software version 12 (trial version)) generated 29 experiments with five central points. Two responses were chosen: Relative Standard Deviation of nanofiber Diameter (RSDD) and TS. RSDD reflects the consistency of film diameter, calculated by dividing the standard deviation of diameter by the average diameter of the measured films (15 points in total). TS of the nanofibers indicates the TS of the films. These responses were employed in a multi-response optimization process. The design order, responses, optimized treatment, and optimized result are presented in Table 1. One treatment was selected for further evaluation based on desirability criteria (achieving the lowest RSDD and the highest TS). Independent variables were tested across various experimental conditions.

Table1: The levels of variables and responses in Box Behnken's design

	Variables				Observed		Predicted	
Treatment number	**A: % BSG in solution**	**B: %acetone in PCL solution**	**C: Voltage**	**D: Distance**	**RSDD**	**TS**	**RSDD**	**TS**
1	25	40	20	15	22.44	0.89	21.77	0.8760
2	10	60	20	15	29.46	0.79	28.29	0.8054
3	40	40	25	15	42.27	0.65	42.04	0.6667
4	10	20	20	15	27.69	0.83	27.04	0.7871
5	25	60	15	15	23.68	0.78	23.64	0.7513
6	25	20	25	15	23.00	0.72	23.49	0.8129
7	25	40	25	18	25.45	0.85	25.56	0.7854
8	10	40	20	18	23.28	0.69	24.29	0.8046
9	25	60	20	18	27.06	0.81	26.63	0.8083
10	25	40	15	18	17.98	0.78	18.59	0.7904
11	10	40	25	15	23.30	0.75	23.14	0.7750
12	25	20	20	18	25.51	0.84	24.70	0.7950
13	25	40	20	15	18.67	0.89	21.77	0.8760
14	25	40	20	15	22.73	0.89	21.77	0.8760
15	25	40	20	15	23.13	0.89	21.77	0.8760
16	25	60	20	12	20.25	0.62	20.84	0.6917
17	25	20	15	15	20.09	0.61	19.90	0.7929
18	25	40	15	12	18.49	0.71	18.15	0.7338
19	40	40	15	15	36.82	0.66	36.76	0.6417
20	40	60	20	15	43.81	0.58	44.22	0.6021
21	10	40	15	15	25.00	0.8	25.02	0.7900
22	25	60	25	15	22.83	0.77	23.46	0.7413
23	25	20	20	12	*18.85*	0.81	*19.07*	*0.8183*
24	40	20	20	15	40.83	0.75	41.76	0.7338
25	10	40	20	12	23.31	0.79	24.24	0.7679
26	25	40	20	15	21.88	0.82	21.77	0.8760
27	40	40	20	18	45.75	0.57	45.27	0.6863
28	25	40	25	12	15.43	0.76	14.59	0.7488
29	40	40	20	12	34.47	0.68	33.91	0.6296
Optimization	20.43	37.80	19.95	14.65	21.69	0.81	20.16	0.88

BSG=Basil Seed Gum; PCL=Polycaprolactone; RSDD=Relative Standard Deviation of nanofiber Diameter; TS=Tensile Strength

Statistical method

Design Expert software version 12 (trial version) was used to optimize the effects of independent parameters on dependent parameters. Statistical analyses were carried out using SPSS Statistics version 26. The data was reported as averages from at least three observations per sample and analyzed using Pair T-Test. *p*-values<0.05 were considered significant throughout this investigation ($p<0.05$).

Results and discussion

Model optimization quality

Table 2 shows the fit statistic of repossess. R^2 was increased by adding model terms. Nevertheless, R^2_{adj} did not increase when insignificant variables were added; indicating the adequacy of the model. In terms of model optimization quality, the lower Coefficient of Variation (CV) indicates better reliability for the experiments. Adequate precision implies that the signal-to-noise is acceptable and a ratio greater than four is desirable. The PRESS indicates how well the model fits each point in the design, with calculated values for RSDD and TS being 68.71 and 0.58, respectively. This metric assesses the capability of the fitted quadratic model for predictive application (Myers et al., 2016).

[DOI: 10.18502/jfqhc.11.4.17441]

Table 2: Fit statistics of dependent variables of optimization stage

Responses	R^2	R^2_{adj}	PRESS	C.V
RSDD	0.98	0.97	68.71	4.68%
TS	0.92	0.84	0.58	3.96%

C.V=Coefficient of Variation; RSDD=Relative Standard Deviation of nanofiber Diameter; TS=Tensile Strength

Optimization of diameter dispersion

Nanofibrous materials can be customized in functionalities by varying their internal structure, surface morphology, and fiber diameter. Due to their much-reduced fiber diameters, nanofibers are easier to use as reinforcement in polymers for producing composite materials with improved mechanical and thermal properties (Park and Rutledge, 2017). Table 3 shows both significant and non-significant effects of independent variables on RSDD according to *p*-values. According to the F values presented in Table 3, variables A and D are the most effective in RSDD. Hence the diameter's dispersion increases with these two parameters' increase. Figure 1a shows that at a voltage of 15 kV, increasing BSG from 10 to 25% resulted in a decrease in nanofiber diameter dispersion, followed by an increasing trend from 25 to 40%.

Table3: ANOVA results and optioned model related to Relative Standard Deviation of nanofiber Diameter (RSDD)

Source	Sum of Squares	df	Mean Square	F-value	*p*-value
Model	1,874.50	14	133.89	88.22	<0.0001
A: % BSG in solution	704.15	1	704.15	463.97	<0.0001
B: %acetone in PCL solution	10.32	1	10.32	6.80	0.0207
C: Voltage	8.70	1	8.70	5.73	0.0312
D: Distance	97.75	1	97.75	64.41	<0.0001
AB	0.3652	1	0.3652	0.2406	0.6314
AC	12.78	1	12.78	8.42	0.0116
AD	31.99	1	31.99	21.08	0.0004
BC	3.56	1	3.56	2.34	0.1480
BD	0.0061	1	0.0061	0.0040	0.9504
CD	27.69	1	27.69	18.25	0.0008
A^2	834.14	1	834.14	549.62	<0.0001
B^2	32.03	1	32.03	21.10	0.0004
C^2	12.12	1	12.12	7.98	0.0135
D^2	9.02	1	9.02	5.95	0.0287
Residual	21.25	14	1.52		
Lack of fit	8.46	10	0.8460	0.2646	0.9599
Pure error	12.79	4	3.20		
Cor total	1,895.75	28			

BSG=Basil Seed Gum; PCL=Polycaprolactone

Variations in RSDD are not drastically affected by varying the voltage across different levels of variable A, indicating that gum concentration within this voltage range greatly influences this response. Conversely, with increasing voltage from 15 to 25 kV, the diameter dispersion increases only slightly across all levels of BSG. Based on this diagram, the optimal voltage is 20 kV. When high voltage is used during electrospinning, the columbic repulsive force within the spinning solution's jet spreads to the viscoelastic solution, and Taylor cone formation stabilizes. Electrospinning critically depends on the voltage supplied to polymer solution; fibers can only be produced when sufficient electrostatic field strength overcomes surface tension at threshold voltage (Bhardwaj and Kundu, 2010). The electric field strength largely influences electrospun fiber diameter; incorrect voltage may result in beaded fibers or mist-like droplets. As shown in Figure 1a, the ideal proportion of BSG is 20.43%. This finding aligns with previous research indicating that polymer solution concentration is a critical variable that impacted bead formation as well as fiber density, shape, and diameter (Jacobs et al., 2010).

Increasing voltage from 15 to 25 kV slightly increases the diameter dispersion in all levels of gum. Our observations indicated that the optimal voltage was 20 kV. When a voltage exceeding the critical value is supplied, the acceleration of charge leads to excess charge release from the needle's tip, causing instability in the Taylor cone. The effects of constant and alternating voltage actuation on the Taylor cone have been studied. The result was consistent with our findings and indicated a critical voltage range (Gupta et al., 2021). Electrospinning is critically dependent on the voltage supplied to the polymer solution. Nevertheless, applying a voltage beyond a certain threshold may lead to instability in the dope jet, accelerating solution-loaded charges and subsequently increasing fiber diameter (Han et al., 2022). One study found that spinning voltage is strongly correlated with bead formation, while solution concentration significantly affects fiber size (Deitzel et al., 2001).

[DOI: 10.18502/jfqhc.11.4.17441]

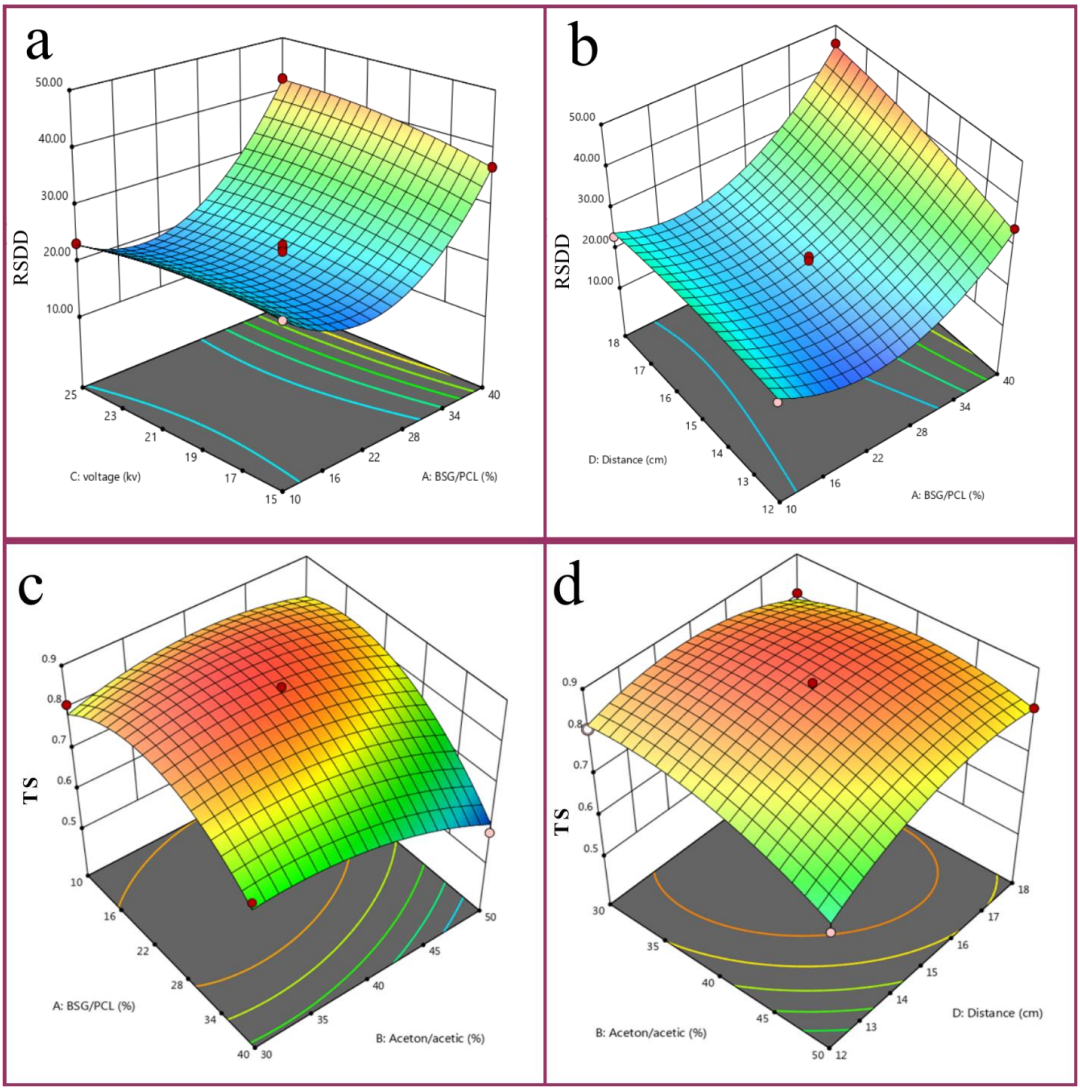

Figure 1: The independent variables' interaction and effect on the dependent variables. (a): The interaction effect of variables Basil Seed Gum (BSG%) and voltage on the Relative Standard Deviation of nanofiber Diameter (RSDD); (b): The interaction effect of variables BSG% and distance on RSDD; (c): The interaction effect of variables BSG and acetone% on Tensile Strength (TS) of nanofibers; (d): Interaction effect of two variables acetone% and distance on TS of nanofibers.

Figure 1b shows that with the increase of gum percentage from 10 to 25% at each distance, RSDD decreased initially but then increases to 40%. According to this graph, the optimal gum concentration and distance are 25% and 12 cm, respectively. By decreasing the distance, RSDD was decreased, and this decrease was more pronounced at 40% gum concentration compared to 10%. Polar or curing distance describes how far the collector is from the needle. It affects electrospun fiber form by varying the degree of solvent volatilization and electric field strength during spinning (Yoon et al., 2018). Determining the critical distance is essential for producing smooth, beadless electrospun fibers (Bhardwaj and Kundu, 2010). Adding a natural polymer into the electrospinning solution reduces viscosity, which in turn leads to reducing fiber diameter (Rashid et al., 2021). However, excessive amounts of natural polymer might increase bead formation. As a polyelectrolyte polymer, natural Basil Seed Mucilage (BSM) polymer can release ionic groups, such as carboxyl into solution. The electrical conductivity of the electrospinning solution is increased by adding anionic and cationic polyelectrolytes (Charles et al., 2021).

Solution viscosity plays a crucial role in defining both the size and form of electrospun fibers. The homogeneous dispersion of solute, influenced by solvent selection, is a crucial determinant in preparing electrospun fibers (Zuo et al., 2005). Smaller diameters and narrower distribution of generated nanofibers result from lower intermolecular forces within solvents and polymers with higher compatibility (Han et al., 2022).

Adding a natural polymer into an electrospinning solution usually results in a decrease in viscosity,

[DOI: 10.18502/jfqhc.11.4.17441]

impacting fibers' morphological structure, and mean dimensions (Rashid et al., 2021). Figure 2 (A2) shows that adding BSG as a natural polymer decreases the diameter of nanofibers. In addition, as can be seen in FE-SEM images, some beads were created in the samples containing BSG. These results were consistent with those of Allafchian et al. (2018), who combined PCL and BSG to produce a biocompatible cell culture scaffold. Kurd et al. (2017) used FE-SEM to show that increasing the BSM ratio in a BSM/Polyvinyl alcohol (PVA) mixture makes the nanofibers thinner. The conductivity of the solution depends on the type of polymer, solvent, and ionic ions. Fiber diameter decreases with increasing solution conductivity and vice versa; high conductivity solutions exhibit significant field instability. Thus wide ranges of dimensions are spread, and electrospinning produces nanofibers with tiny diameters (Xue et al., 2019).

Optimization of TS

According to the F values (Table 4), two variables, A and B, have the most significant effect on TS. As shown in Figure 1c, across all levels of variable B, TS increased by decreasing the gum percentage from 40 to 25%; however, this trend subsequently declined. Moreover, with the increase of acetone percentage up to 40% across all levels of variable A, an initial increase in TS occurred followed by a decrease. Furthermore, films exhibited peak TS values at 40% acetone and 25% gum concentration. Figure 1d illustrates that when investigating the effects of variables B and D, reducing acetone concentration up to 40% at a distance of 12 cm increased TS, then it decreased gradually. At a distance of 18 cm, a similar trend was observed, but with minimal amounts of alterations. This three-dimensional diagram indicates the optimal TS at a concentration of 40% acetone.

Table4: ANOVA table and optioned model related to Tensile Strength (TS) of nanofiber diameter

Source	Sum of Squares	df	Mean Square	F-value	*p*-value
Model	0.1593	14	0.0114	12.22	<0.0001
A: % BSG in solution	0.0494	1	0.0494	53.09	<0.0001
B: %acetone in PCL solution	0.0096	1	0.0096	10.35	0.0062
C-voltage	0.0001	1	0.0001	0.0806	0.7806
D-Distance	0.0065	1	0.0065	7.02	0.0190
AB	0.0056	1	0.0056	6.04	0.0276
AC	0.0004	1	0.0004	0.4298	0.5227
AD	0.0001	1	0.0001	0.1075	0.7479
BC	0.0002	1	0.0002	0.2418	0.6305
BD	0.0049	1	0.0049	5.27	0.0377
CD	0.0001	1	0.0001	0.1075	0.7479
A^2	0.0650	1	0.0650	69.82	<0.0001
B^2	0.0125	1	0.0125	13.39	0.0026
C^2	0.0215	1	0.0215	23.11	0.0003
D^2	0.0188	1	0.0188	20.20	0.0005
Residual	0.0130	14	0.0009		
Lack of fit	0.0091	10	0.0009	0.9294	0.5817
Pure error	0.0039	4	0.0010		
Cor total	0.1723	28			

BSG=Basil Seed Gum; PCL=Polycaprolactone

Choosing the solvents based on their charge densities in the solution allows one to regulate the interaction between solvent and polymer molecules, which in turn defines solution viscosity. However, using solvents can cause thermodynamic instability in polymer solutions, resulting in holes developing in fibers as solvent evaporates entirely from areas with high solvent concentrations. Our result indicated that TS in a 50% acetone solution increased as distance grew from 12 to 15 cm (Figure 1d), but then decreased up to a distance of 18 cm. A similar trend was observed at 30% acetone, indicating that 15 cm is the optimal distance for maximizing TS values. It is essential to maintain an appropriate gap between the spinneret and the collection. A distance too large might prevent the ejected solution from reaching the collectors. Our result align with those of Ding et al. (2019), who reported that as the spinning distance increases, so does TS of electrospun fiber; however, the fiber diameter decreases.

Multi-response and variable optimization

Investigating multi-response properties through desirability analysis is one of the most effective optimization techniques. This approach is based on the notion that a quality process possesses specific quality traits. Within this framework, we sought a compromise among multiple responses (Lee et al., 2020). The expected averages for two dependent variables fall between upper and lower limits of Prediction Interval (PI), which confirms the accuracy of the process based on data presented in Table 5. The last stage of the procedure is to forecast and validate performance characteristic after choosing optimal levels for electrospinning parameters.

[DOI: 10.18502/jfqhc.11.4.17441]

The trial run were carried out using the ideal parameter settings mentioned above, aimed at optimizing fiber diameter and bead number. Results were then compared with acquired optimal response values to validate the created models. The experimental findings show a TS of 0.88 and a fiber diameter of 20.16 nm, respectively. The error percentage for experimental validation of constructed models at optimum parameters is presented in Table 5. The software selected the desirability of one treatment, revealing that BSG gum had the most significant effect on both responses. Confirmation processes are utilized to verify that the model can accurately predict real-world outcomes using the optimal settings derived from this research. A PI defines upper and lower limits within which future sample averages are expected to fall (Stevens and Anderson-Cook, 2019). Since prediction intervals have to account for the unidentified variance of a sample, they will be larger than the confidence intervals. Whereas confidence intervals are for population averages (an infinite sample), prediction intervals are for averages from small samples (Jensen, 2016).

Table 5: Conformation and Prediction Interval (PI) values of multi-response and variable optimization

Solution 1	Predicted Mean	observed	SD	n	SE Pred	95% PI low	95% PI high
RSDD	20.16	21.34	1.23	1	1.34	17.28	23.04
TS	0.885473	0.83	0.0305057	1	0.0332169	0.81423	0.956717

RSDD=Relative Standard Deviation of nanofiber Diameter; SD=Standard Deviation;
SE Pred=Standard Error of Prediction; TS=Tensile Strength

AFM results

The AFM test results for the samples are shown in Figure 2. Evidence indicates that including BSG in PCL increases the roughness of the film's surface. AFM has proven to be a valuable tool for investigating nanostructure alterations and examining nano-mechanical characteristics. It has been observed that increasing BSG concentration leads to an increase in roughness; similar results were reported by (Oraç et al., 2023). The skew profile shows the porosity and load-bearing capacity of surfaces. A negative skewness value is the most trustworthy indication of a bearing surface (Rajesh Kumar and Subba RAO, 2012), while a higher positive skewness value suggests a greater occurrence of bumps. When the value of coefficient of kurtosis (Ska) is below three, the distribution is described as platykurtic, indicating a subtle peak. Moreover, when the value of Ska exceeds three, the distribution is characterized as leptokurtic, suggesting a pronounced peak (Egbu et al., 2022). In all samples, Ska was greater than three, indicating their distribution was leptokurtic, with negative skewness in all of them being a sign of more cavities.

ATR-FTIR observation

Accurate measurement and characterization of polymer materials are achievable through ATR-FTIR techniques. Figure 3a displays its spectra for sample films. ATR-FTIR spectroscopy was conducted at ambient temperature across a range of 450-4,000 1/cm to identify interactions between PCL and BSG within the polymer matrix. Anticipated interactions between these components typically involve the formation of hydrogen bonds between the C-O groups of PCL and the O-H groups of BSG. The stretching C=O, C-O from carboxylic acid, and C-O-C correspond to the many peaks on the PCL curve that can be seen in 1,720, 1,295, and 1,160 1/cm regions (Figure $3A_1$), which was corroborated by other studies (Li et al., 2022). $A_{2,}$ peaks shown in Figure 3a, may relate to BSG addition. Previous studies suggest that the structure of PCL and BSG indicates that the peaks around 2360 1/cm most likely arise from the bond between C-O from PCL and O-H from BSG (Schneller et al., 2013). However, some research has reported no chemical bond between PCL and BSM (Allafchian et al., 2018). Combining different materials with PCL alters its crystallinity and thermal behavior. Lower temperatures and more frequent weight loss rates are promoted by adding BSG to PCL due to its greater moisture content. Thermal breakdown investigations indicate that PCL's thermal stability is reduced when BSG is included within film composition.

[DOI: 10.18502/jfqhc.11.4.17441]

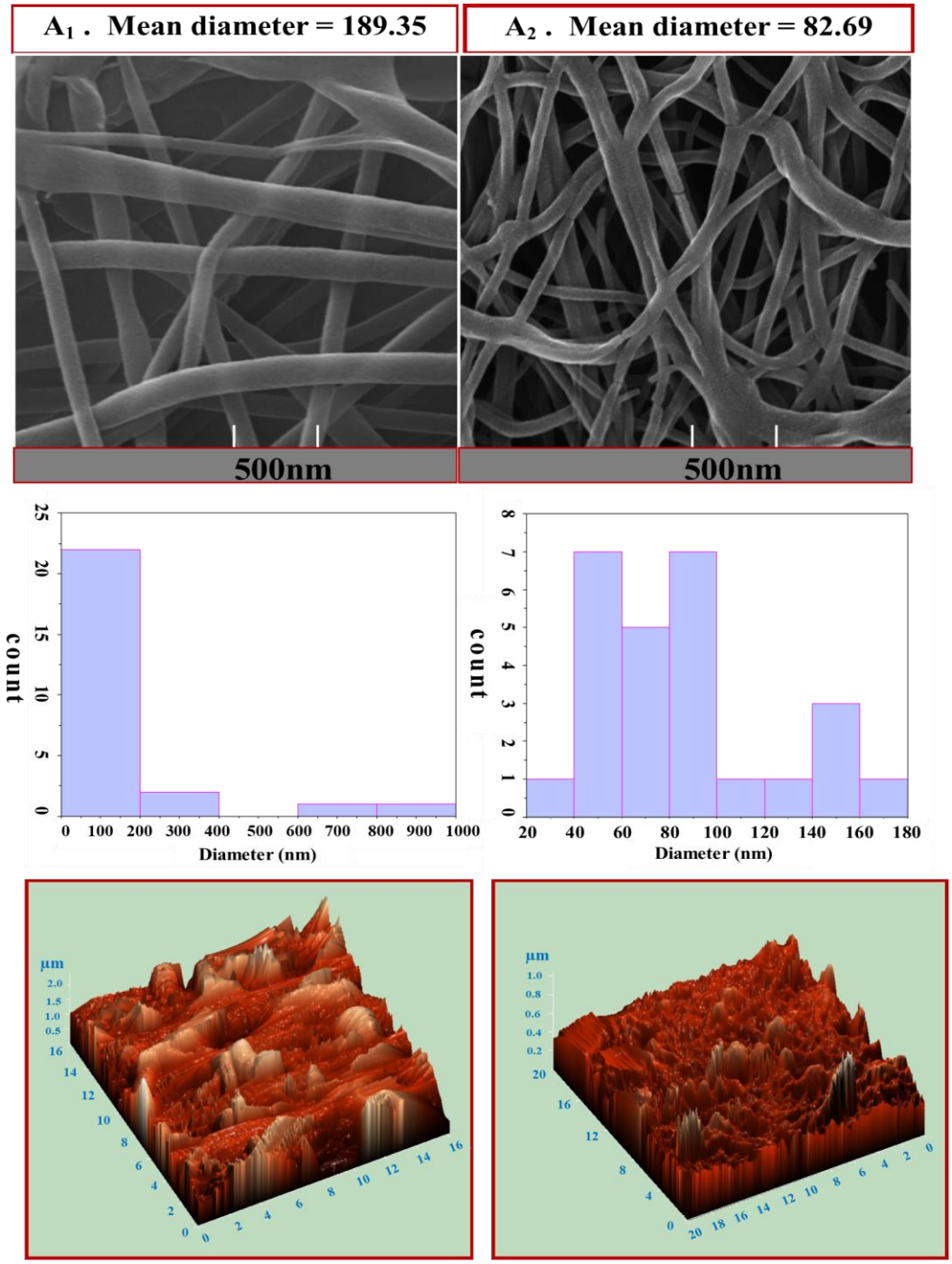

Figure 2: Field Emission-Scanning Electron Microscopy (FE-SEM) micrographs, diameter distribution histograms, and Atomic Force Microscope (AFM) of the electrospun nanofibers.
A_1: PCL; A_2: PCL 90%+BSG 10%
BSG=Basil Seed Gum; PCL=Polycaprolactone

[DOI: 10.18502/jfqhc.11.4.17441]

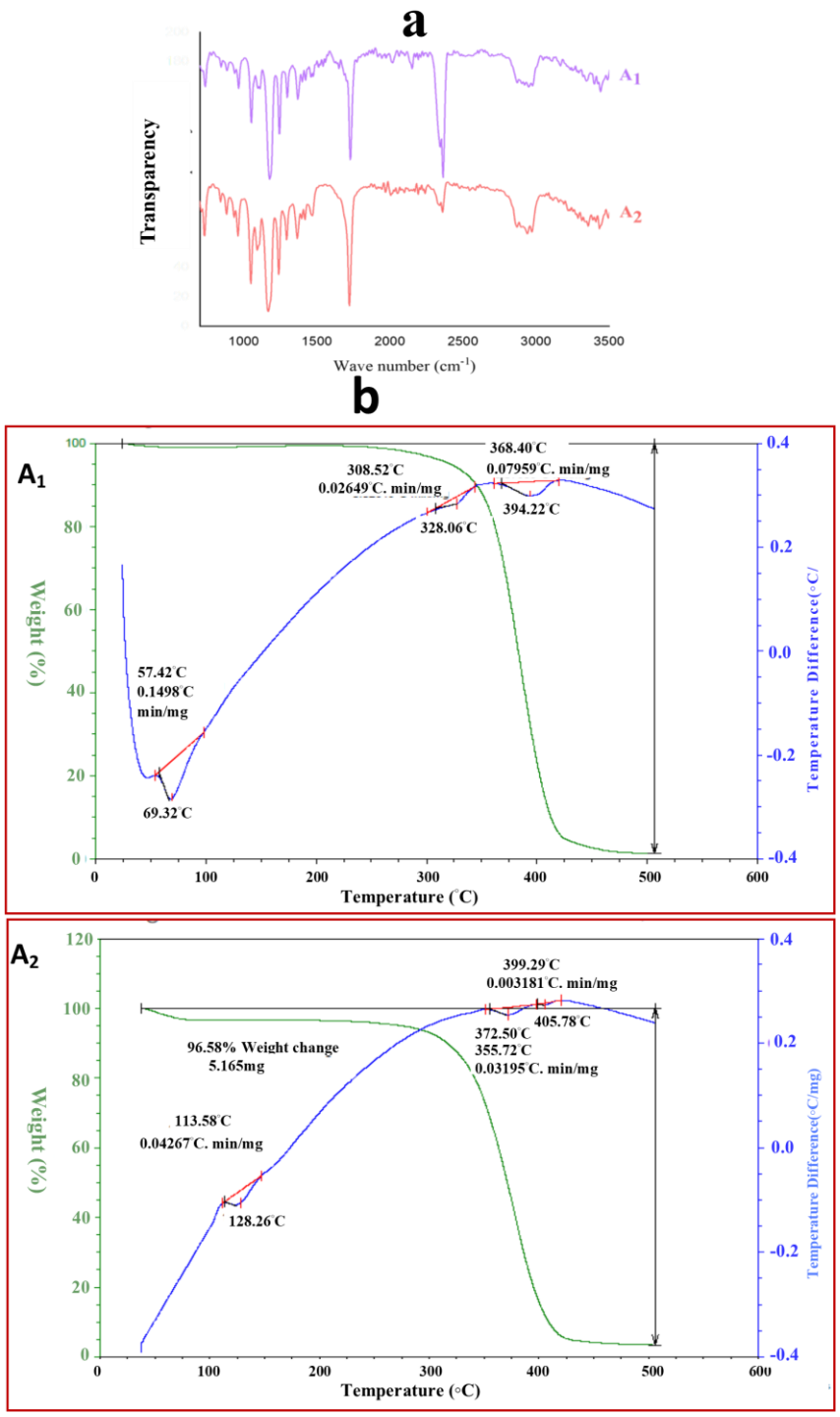

Figure 3: (a) Attenuated Total Reflectance- Fourier Transform Infrared spectroscopy (ATR-FTIR) of the electrospun nanofibers; (b) Thermal Gravimetric Analysis-Differential Thermal Analysis (TGA-DTA) of the electrospun nanofibers.
A_1: PCL. A_2: PCL 90%+BSG 10%
BSG=Basil Seed Gum; PCL=Polycaprolactone

Thermogravimetry Differential Thermal Analysis (TG/DTA) results

As shown in Figure 3b, sample A_1 initially lost weight at 50 ºC, followed by another lossat 325 ºC. Significant weight loss was observed between 350 and 410 ºC, and by 475 ºC, the breakdown process was concluded. A_2 sample's weight first starts to decline at about 35 ºC, with a subsequent drop occurring at 300 ºC and a complete breakdown at 425 ºC. DTA results are also shown in Figure 3b. Sample A_1 displayed two endothermic reactions at 69

[DOI: 10.18502/jfqhc.11.4.17441]

and 394 ºC, along with one exothermic reaction at 350 ºC. Sample A_2 exhibited two endothermic reactions at 128 and 405 ºC.

Thickness, WVP, and OTR results

The measured film thicknesses are presented in Table 6. The inclusion of BSG resulted in a significant decrease in film thickness (p<0.05). Furthermore, incorporating BSG caused an insignificant reduction in PCL's TS (p<0.05). The results were consistent with those reported by Allafchian et al. (2018), who combined PCL and BSG to create biocompatible scaffolds for cell culture applications. Similarly, Cesur (2018) found that adding a natural polymer weakens the structure. Table 6 shows the inclusion of BSG into PCL and its effect on WVP and OTR properties. This Table indicates a significant increase (p<0.05) in the WVP for the sample containing BSG, while other measured variables, including OTR, thickness, and TS, were significantly reduced (p<0.05). Specifically, Adding BSG into PCL considerably increased WVP (p<0.05), which can depend on the film's thickness, surface behavior, crystallinity, and integrity. The hydrophilic elements and porous structure of the film contribute to elevating WVP. The polysaccharide molecules rich in hydroxyl groups enhance both BSG content and WVP (Hashemi Gahruie et al., 2019). As illustrated in Table 6, adding gum to PCL significantly reduced OTR by almost 50%. Oxygen permeates more readily through PCL due to its hydrophobic nature. One study indicated that biopolymers such as chitosan, cellulose derivatives, milk proteins, and alginate exhibit lower oxygen permeability than synthetic polymeric films like PCL, polypropylene, and polyethylene (Azeredo et al., 2009). Additionally, in some studies, reduction in OTR for biofilms made with BSG was reported (Shahrajabian et al., 2020). Numerous hydrogen bonds formed by hydroxyl groups within biopolymer films contribute to their hydrophilic characteristics. These hydrogen bonds likely act as efficient barriers against non-polar molecules like oxygen.

Table 6: The comparison between Water Vapor Permeability (WVP), Oxygen Transmission Rate (OTR), thickness, and Tensile Strength (TS) values of the prepared samples

Samples	WVP ($g/(m.h.Pa))\times10^{-10}$	OTR ($cc/cm^2.min.mbar$)	Thickness (nm)	TS (Mpa)
A_1	200±10.4 [a]	12.6±1.31 [a]	108±34.03 [a]	2.27±0.16 [a]
A_2	940±50 [b]	6.1±0.72 [b]	78±14.43 [b]	0.81±0.04 [a]

BSG=Basil Seed Gum; PCL=Polycaprolactone
A_1: PCL; A_2: PCL 90%+BSG 10%
Different letters in the same column indicate significant differences (p<0.05).

Conclusion

Composite nanofibers made from PCL and BSG exhibit enhanced properties regarding oxygen permeability and superior biocompatibility, making them suitable for packaging foods that are low in moisture and susceptible to oxygen exposure. Based on ANOVA results for RSDD, the percentage of BSG in solution (A), Distance (D), and TS, it was determined that variables A and the percentage of acetone in PCL solution (B) were the most effective parameters. Confirmation results indicated that the predicted mean for RSDD and TS responses fell within acceptable; therefore validating the used method. The addition of BSG caused a significant increase in WVP; however, it reduced the films' TS, OTR, and thickness, with these decreases being significant except for TS. TGA test results indicated a reduction in thermal stability as well. Additionally, increased roughness was observed in the 3D AFM photographs of BSG samples. Our research indicates that BSG is a gum with inadequate electrospinning capabilities. Future research should explore the combination of BSG with other biodegradable polymers, such as PVA and poly (lactic acid), as well as incorporating natural preservatives.

Author contributions

V.G.-M. and E.S. designed the study; N.Z. conducted the experimental work; V.G.-M. and A.F.-N. analyzed the data; V.G.-M and N.Z. wrote the manuscript. All authors read and approved the final manuscript.

Conflicts of interest

The authors declare that there is no conflict of interest .

Acknowledgments

The authors would like to thank the Hamadan University of Medical Science, Hamadan, Iran, for the financial support

Funding

This study has been adapted from an MSc thesis, and the Vice-Chancellor funded it for Research and Technology, Hamadan University of Medical Sciences (No. 1401120910673).

[DOI: 10.18502/jfqhc.11.4.17441]

Ethical consideration

Not applicable.

References

Adibi A., Trinh B.M., Mekonnen T.H. (2023). Recent progress in sustainable barrier paper coating for food packaging applications. *Progress in Organic Coatings*. 181: 107566. [DOI: 10.1016/j.porgcoat.2023.107566]

Allafchian A.R., Seyed Jalali A.H., Seyed Mousavi E. (2018). Biocompatible biodegradable polycaprolactone/basil seed mucilage scaffold for cell culture. *IET nanobiotechnology*. 12: 1003-1149. [DOI: 10.1049/iet-nbt.2018.5071]

American Society for Testing and Materials (ASTM). (2005). Standard test methods for water vapor transmission of materials. *ASTM International*. URL: https://www.astm.org/e0096-00.html.

ASTM International. (2005). Standard test methods for water vapor transmission of materials. ASTM E96/E96M-2005. URL: https://cdn.standards.iteh.ai/samples/41444/ee99c0b797cc4ae1a9f6d85416ae1302/ASTM-E96-E96M-05.pdf.

Azeredo H.M.C., Mattoso L.H.C., Wood D., Williams T.G., Avena-Bustillos R.J., McHugh T.H. (2009). Nanocomposite edible films from mango puree reinforced with cellulose nanofibers. *Journal of Food Science*. 74: N31-N35. [DOI: 10.1111/j.1750-3841.2009.01186.x]

Beikzadeh S., Khezerlou A., Seid Jafari M., Pilevar Z., Mortazavian A.M. (2020). Seed mucilages as the functional ingredients for biodegradable films and edible coatings in the food industry. *Advances in Colloid and Interface Science*. 280: 102164. [DOI: 10.1016/j.cis.2020.102164]

Bhardwaj N., Kundu S.C. (2010). Electrospinning: a fascinating fiber fabrication technique. *Biotechnology Advances*. 28: 325-347. [DOI: 10.1016/j.biotechadv.2010.01.004]

Biswas S., Bal M., Behera S.K., Sen T.K., Meikap B.C. (2019). Process optimization study of Zn^{2+} adsorption on biochar-alginate composite adsorbent by Response Surface Methodology (RSM). *Water*. 11: 325. [DOI: 10.3390/w11020325]

Cazón P., Morales-Sanchez E., Velazquez G., Vázquez M. (2022). Measurement of the water vapor permeability of chitosan films: a laboratory experiment on food packaging materials. *Journal of Chemical Education*. 99: 2403-2408. [DOI: 10.1021/acs.jchemed.2c00449]

Cesur S. (2018). The effects of additives on the biodegradation of polycaprolactone composites. *Journal of Polymers and the Environment*. 26: 1425-1444. [DOI: 10.1007/s10924-017-1029-y]

Charles A.P.R., Jin T.Z., Mu R., Wu Y. (2021). Electrohydrodynamic processing of natural polymers for active food packaging: a comprehensive review. *Comprehensive Reviews in Food Science and Food Safety*. 20: 6027-6056. [DOI: 10.1111/1541-4337.12827]

Deitzel J.M., Kleinmeyer J., Harris D., Beck Tan N.C. (2001). The effect of processing variables on the morphology of electrospun nanofibers and textiles. *Polymer*. 42: 261-272. [DOI: 10.1016/S0032-3861(00)00250-0]

Ding C., Fang H., Duan G., Zou Y., Chen S., Hou H. (2019). Investigating the draw ratio and velocity of an electrically charged liquid jet during electrospinning. *RSC Advances*. 9: 13608-13613. [DOI: 10.1039/c9ra02024a]

Egbu J., Ohodnicki P.R., Baltrus J.P., Talaat A., Wright R.F., McHenry M.E. (2022). Analysis of surface roughness and oxidation of FeNi-based metal amorphous nanocomposite alloys. *Journal of Alloys and Compounds*. 912: 165155. [DOI: 10.1016/j.jallcom.2022.165155]

Ferreira S.L.C., Bruns R.E., Ferreira H.S., Matos G.D., David J.M., Brandão G.C., Da Silva E.G.P., Portugal L.A., Dos Reis P.S., Souza A.S., Dos Santos W.N.L. (2007). Box-Behnken design: an alternative for the optimization of analytical methods. *Analytica Chimica Acta*. 597: 179-186. [DOI: 10.1016/j.aca.2007.07.011]

Gupta A., Mishra B.K., Panigrahi P.K. (2021). Internal and external hydrodynamics of Taylor cone under constant and alternating voltage actuation. *Physics of Fluids*. 33: 117118. [DOI: 10.1063/5.0071921]

Han W., Wang L., Li Q., Ma B., He C., Guo X., Nie J., Ma G. (2022). A review: current status and emerging developments on natural polymer-based electrospun fibers. *Macromolecular Rapid Communications*. 43: 2200456. [DOI: 10.1002/marc.202200456]

Hashemi Gahruie H., Eskandari M.H., Van Der Meeren P., Seyed Hosseini M.H. (2019). Study on hydrophobic modification of basil seed gum-based (BSG) films by octenyl succinate anhydride (OSA). *Carbohydrate Polymers*. 219: 155-161. [DOI: 10.1016/j.carbpol.2019.05.024]

Hashemi Gahruie H., Ziaee E., Eskandari M.H., Seyed Hosseini M.H. (2017). Characterization of basil seed gum-based edible films incorporated with *Zataria multiflora* essential oil nanoemulsion. *Carbohydrate Polymers*. 166: 93-103. [DOI: 10.1016/j.carbpol.2017.02.103]

International Standard Organization (ISO). (2007). Plastics - film and sheeting - determination of gas-transmission rate - part 1: differential-pressure method. ISO 15105-1:2007.. Geneva, Switzerland. URL: https://cdn.standards.iteh.ai/samples/41677/ba5642d6d50d46d4a8a0b71df1ab2ee3/ISO-15105-1-2007.pdf.

Jacobs V., Anandjiwala R.D., Maaza M. (2010). The influence of electrospinning parameters on the structural morphology and diameter of electrospun nanofibers. *Journal of Applied Polymer Science*. 115: 3130-3136. [DOI: 10.1002/app.31396]

Janani N., Zare E.N., Salimi F., Makvandi P. (2020). Antibacterial tragacanth gum-based nanocomposite films carrying ascorbic acid antioxidant for bioactive food packaging. *Carbohydrate Polymers*. 247: 116678. [DOI: 10.1016/j.carbpol.2020.116678]

Jensen W.A. (2016). Confirmation runs in design of experiments. *Journal of Quality Technology*. 48: 162-177. [DOI: 10.1080/00224065.2016.11918157]

Jouki M., Khazaei N., Ghasemlou M., HadiNezhad M. (2013). Effect of glycerol concentration on edible film production from cress seed carbohydrate gum. *Carbohydrate Polymers*. 96: 39-46. [DOI: 10.1016/j.carbpol.2013.03.077]

Kurd F., Fathi M., Shekarchizadeh H. (2017). Basil seed mucilage as a new source for electrospinning: production and physicochemical characterization. *International Journal of*

[DOI: 10.18502/jfqhc.11.4.17441]

Biological Macromolecules. 95: 689-695. [DOI: 10.1016/j.ijbiomac.2016.11.116]

Lee D.-H., Kim S.-H., Byun J.-H. (2020). A method of steepest ascent for multiresponse surface optimization using a desirability function method. *Quality and Reliability Engineering International*. 36: 1931-1948. [DOI: 10.1002/qre.2666]

Li T., Zhang X., Mei J., Cui F., Wang D., Li J. (2022). Preparation of linalool/polycaprolactone coaxial electrospinning film and application in preserving salmon slices. *Frontiers in Microbiology*. 13: 860123 [DOI: 10.3389/fmicb. 2022. 860123]

Lo Faro E., Bonofiglio A., Barbi S., Montorsi M., Fava P. (2023). Polycaprolactone/starch/agar coatings for food-packaging paper: statistical correlation of the formulations' effect on diffusion, grease resistance, and mechanical properties. *Polymers*. 15: 3921. [DOI: 10.3390/polym15193921]

Min T., Zhou L., Sun X., Du H., Zhu Z., Wen Y. (2022). Electrospun functional polymeric nanofibers for active food packaging: a review. *Food Chemistry*. 391: 133239. [DOI: 10.1016/j.foodchem.2022.133239]

Mirhosseini H., Amid B.T. (2012). A review study on chemical composition and molecular structure of newly plant gum exudates and seed gums. *Food Research International*. 46: 387-398. [DOI: 10.1016/j.foodres.2011.11.017]

Mittal V. (2011). Polymers from renewable resources. In: Mittal V. (Editor). Renewable polymers: synthesis, processing, and technology. Scrivener Publishing, Texas, USA. pp: 1-22. [DOI: 10.1002/9781118217689]

Mohammadi A., Ghasemzadeh-Mohammadi V., Haratian P., Khaksar R., Chaichi M. (2013). Determination of polycyclic aromatic hydrocarbons in smoked fish samples by a new microextraction technique and method optimisation using response surface methodology. *Food Chemistry*. 141: 2459-2465. [DOI: 10.1016/j.foodchem.2013.05.065]

Myers R.H., Montgomery D.C., Anderson-Cook C.M. (2016). Response surface methodology: process and product optimization using designed experiments. 4th edition. John Wiley and Sons. New York, USA.

Nazir S., Wani I.A. (2021). Physicochemical characterization of basil (*Ocimum basilicum* L.) seeds. *Journal of Applied Research on Medicinal and Aromatic Plants*. 22: 100295. [DOI: 10.1016/j.jarmap.2021.100295]

Nemat B., Razzaghi M., Bolton K., Rousta K. (2019). The Role of food packaging design in consumer recycling behavior—a literature review. *Sustainability*. 11: 4350. [DOI: 10.3390/su11164350]

Oraç A., Konak Göktepe Ç., Demirci T., Akın N. (2023). Biodegradable edible film based on basil seed gum: the effect of gum and plasticizer concentrations. *Journal of Polymers and the Environment*. 31: 5003-5014. [DOI: 10.1007/s10924-023-02923-w]

Pan J., Ai F., Shao P., Chen H., Gao H. (2019). Development of polyvinyl alcohol/β-cyclodextrin antimicrobial nanofibers for fresh mushroom packaging. *Food Chemistry*. 300: 125249. [DOI: 10.1016/j.foodchem.2019.125249]

Park J.H., Rutledge G.C. (2017). 50th anniversary perspective: advanced polymer fibers: high performance and ultrafine. *Macromolecules*. 50: 5627-5642. [DOI: 10.1021/acs.macromol.7b00864]

Rajesh Kumar B., Subba RAO T. (2012). AFM studies on surface morphology, topography and texture of nanostructured zinc aluminum oxide thin films. *Digest Journal of Nanomaterials and Biostructures (DJNB)*. 7: 1881-1889.

Rashid T.U., Gorga R.E., Krause W.E. (2021). Mechanical Properties of electrospun fibers—a critical review. *Advanced Engineering Materials* 23: 2100153. [DOI: 10.1002/adem.202100153]

Sarabia L.A., Ortiz M.C. (2009). Response surface methodology. In: Brown S.D., Tauler R., Walczak B. (Editors.). Comprehensive chemometrics: chemical and biochemical data analysis. Elsevier, Amsterdam, Netherlands. pp: 345-390. [DOI: 10.1016/B978-044452701-1.00083-1]

Schneller T., Waser R., Kosec M., Payne D. (2013). Chemical solution deposition of functional oxide thin films. 1st edition. Springer, Vienna. pp: 1-796.

Sen S., Bal T., Rajora A.D. (2022). Green nanofiber mat from HLM-PVA-Pectin (*Hibiscus* leaves mucilage-polyvinyl alcohol-pectin) polymeric blend using electrospinning technique as a novel material in wound-healing process. *Applied Nanoscience*. 12: 237-250. [DOI: 10.1007/s13204-021-02295-4]

Shahrajabian M.H., Sun W., Cheng Q. (2020). Chemical components and pharmacological benefits of basil (*Ocimum basilicum*): a review. *International Journal of Food Properties*. 23: 1961-1970. [DOI: 10.1080/10942912.2020.1828456]

Stevens N.T., Anderson-Cook C.M. (2019). Design and analysis of confirmation experiments. *Journal of Quality Technology*. 51: 109-124. [DOI: 10.1080/00224065.2019.1571344]

Suganthi S., Vignesh S., Kalyana Sundar J., Raj V. (2020). Fabrication of PVA polymer films with improved antibacterial activity by fine-tuning via organic acids for food packaging applications. *Applied Water Science*. 10: 100. [DOI: 10.1007/s13201-020-1162-y]

Thakur M., Majid I., Hussain S., Nanda V. (2021). Poly (ε- caprolactone): a potential polymer for biodegradable food packaging applications. *Packaging Technology and Science*. 34: 449-461. [DOI: 10.1002/pts.2572]

Wandosell G., Parra-Meroño M.C., Alcayde A., Baños R. (2021). Green packaging from consumer and business perspectives. *Sustainability*. 13: 1356. [DOI: 10.3390/su13031356]

Xue J., Wu T., Dai Y., Xia Y. (2019). Electrospinning and electrospun nanofibers: methods, materials, and applications. *Chemical Reviews*. 119: 5298-5415. [DOI: 10.1021/acs.chemrev.8b00593]

Yoon J., Yang H.-S., Lee B.-S., Yu W.-R. (2018). Recent progress in coaxial electrospinning: new parameters, various structures, and wide applications. *Advanced Materials*. 30: 1704765. [DOI: 10.1002/adma.201704765]

Zuo W., Zhu M., Yang W., Yu H., Chen Y., Zhang Y. (2005). Experimental study on relationship between jet instability and formation of beaded fibers during electrospinning. *Polymer Engineering and Science*. 45: 704-709. [DOI: 10.1002/pen.20304]

[DOI: 10.18502/jfqhc.11.4.17441]